



Front-face synchronous fluorescence spectroscopy: a rapid and non-destructive authentication method for Arabica coffee adulterated with maize and soybean flours

Jing-Ya Xie¹ · Jin Tan¹

Received: 17 April 2022 / Revised: 6 July 2022 / Accepted: 26 July 2022 / Published online: 17 August 2022
© Bundesamt für Verbraucherschutz und Lebensmittelsicherheit (BVL) 2022

Abstract

This article describes a novel front-face synchronous fluorescence spectroscopy (FFSFS) method for the fast and non-invasive authentication of ground roasted Arabica coffee adulterated with roasted maize and soybean flours. The detection was based on the different composition of fluorescent Maillard reaction products and caffeine in roasted coffee and cereal flours. For each roasted maize or soybean adulterant flour (5–40 wt%), principal component analysis coupled with linear discriminant analysis (PCA–LDA) was used for qualitative discrimination. Quantitative prediction models were constructed based on the combination of unfolded total synchronous fluorescence spectra and partial least square regression (PLSR), followed by fivefold cross-validation and external validation. The PLSR models produced suitable results, with the determination coefficient of prediction (R_p^2) > 0.9, root mean square error of prediction (RMSEP) < 5%, relative error of prediction (REP) < 25% and residual predictive deviation (RPD) > 3. The limits of detection (LOD) were both 10% for roasted maize and soybean flours. Most relative errors for the prediction of simulated blind samples were between -30% and +30%. The benefits of this strategy are simplicity, rapidity, and non-destructive detection. However, owing to the high similarity between roasted coffee and roasted cereal flours and the influence of the roasting degree on fluorescent Maillard reaction products, its application is limited to the preliminary screening of roasted coffee with the same roasting degree, adulterated with relatively large amounts of roasted cereal flours which are roasted to analogous color to the coffee.

Keywords Coffee adulteration · Roasted cereal flour · Food fraud · Spectrofluorimetry · Principal component analysis · Linear discriminant analysis

1 Introduction

Coffee is the most popular and the most consumed beverage worldwide (Bilge 2020). In the past decade, along with the surge of consumer demands and the rapid development of coffee markets, coffee has become the second largest commodity after oil (Ebrahimi-Najafabadi et al. 2012). Its huge profit margin has spawned many adulterations, especially for coffee Arabica which is recognized to be aromatically superior and commercially more valuable compared to other coffee cultivars (Danezis et al. 2016a, b; Toci et al. 2016).

The adulteration of roasted coffee is diverse, impurities and the addition of low-cost substances are the most common maneuver of adulteration (Domingues et al. 2014; Reis et al. 2013a; Toci et al. 2016). One of the most common adulterants in ground roasted coffee is roasted cereal flour such as maize and soybean flours (Arrieta et al. 2019; Cai et al. 2016; Daniel et al. 2018; Toci et al. 2016). Since various biological substances present similar physio-chemical characteristics after roasting, the high resemblance of these roasted flours to ground roasted coffee makes it a great challenge to identify this fraud (Reis et al. 2013b).

Conventional methods to identify the adulteration of ground roasted coffee involve optical and electron microscopy which require considerable technical ability (Toci et al. 2016; Wang et al. 2020). Other instrumental techniques including chromatographic methods and mass spectroscopy are more reliable, reproducible and widely applicable (Domingues et al. 2014; Cai et al. 2016; Daniel et al. 2018;

✉ Jin Tan
tanjin@tjcu.edu.cn

¹ Tianjin Key Laboratory of Food Biotechnology, College of Biotechnology and Food Science, Tianjin University of Commerce, Tianjin 300134, People's Republic of China

Garrett et al. 2012; Toci et al. 2016). However, they usually require pretreatment of samples and are complicated and time-consuming. In contrast, spectral methods, especially vibrational spectroscopic techniques such as Fourier transform near-infrared (FT-NIR) (Ebrahimi-Najafabadi et al. 2012; Chakravartula et al. 2022) and Fourier transform mid-infrared (FT-MIR) (Reis et al. 2017, 2013a, b) spectroscopies provide convenient procedures for the authentication of coffee without or with simple sample pretreatment (Toci et al. 2016).

Fluorescence spectroscopy is known for its high sensitivity and selectivity, though it is not as popular as the aforementioned vibrational spectroscopic techniques (Danezis et al. 2016a, b). In recent years, the combined use of fluorescence spectroscopy with multivariate statistical analysis has increasingly been used for food authentication (Callao and Ruisánchez 2018). It has shown great potential in the authentication of various kinds of foods and beverages (Karoui and Blecker 2011).

With respect to coffee, its fluorescent property has been investigated, however, only limited to the aqueous extraction of green coffee. For instance, Botelho et al. (2017) achieved the qualitative classification of coffees produced in Brazil according to the geographical origin. Yisak et al. (2018) developed a fluorescent method for the simultaneous determination of trigonelline and theobromine in the aqueous extract of green coffee beans. Compared to green coffee, roasted coffee is a completely different situation. During roasting, a number of biological materials are oxidized and react with each other while a large quantity of aromatic compounds and Maillard reaction products are produced (Reis et al. 2013b). Hence, dramatic changes are expected to occur to the fluorescent properties of coffee. However, to the best of our knowledge, neither the fluorescent characteristics of roasted coffee nor the quantitative authentication of coffee adulteration with roasted cereal flours by using fluorescence spectroscopy has been reported.

Herein, FFSFS which directly monitors the fluorescent excitation and emission on the surface of samples simultaneously was utilized to compare the fluorescent properties of ground roasted Arabica coffee and two common adulterants in ground roasted coffee, namely roasted maize and soybean flours. The aim of this study was to reveal the fluorescent characteristics of roasted coffee, to find out whether the highly resembling roasted cereal flours and ground roasted coffee can be discerned by FFSFS, and to test the feasibility of using it to authenticate coffee adulteration with roasted cereal flours.

2 Material and methods

2.1 Samples and chemicals

Six commercial brands of medium roasted Arabica coffee (*Coffea arabica*) from Brazil, Cuba, Colombia, and Italy were purchased from online markets. Either roasted Arabica coffee beans or ground roasted Arabica coffee samples were collected. Five commercial brands of maize flour and six brands of soybean flour produced in China were also obtained from online markets. The coffee beans for the production of the above roasted coffee samples and the cereals were harvested in 2019 and 2020. All samples were kept at 4 °C in the dark prior to analysis. The authenticity of these samples was guaranteed by the certified manufacturers and online sellers. Caffeine of analytical grade (> 99%) was purchased from Aladdin Reagent Co., Ltd. (Shanghai, China).

Prior to analysis, the roasted coffee beans were ground into fine powders by an IKA M20 universal mill (IKA, Königswinter, Germany). Ground coffee and cereal flours were passed through a sieve (mesh 250 µm). The five brands of maize flour samples from different origins were mixed homogeneously. Analogous operation was made for the six brands of soybean flours. Consequently, two representative mixed maize and soybean flours were obtained and then roasted under different conditions to give similar appearance to the roasted coffee samples. The roasting temperature and time for maize and soybean flours were 240 °C for 30 min and 220 °C for 40 min, respectively. The above process yielded roasted maize and soybean flours of similar luminosity (L^*) to the collected roasted coffee samples, which were all medium roasted ($21.0 < L^* < 23.5$) (Reis et al. 2017; 2013b). Color measurements were performed using a colorimeter (UltraScan Pro Spectrophotometer, Hunter Laboratories, VA, USA) with standard D65 illumination.

For the preparation of adulterated coffee samples, binary blends containing ground roasted coffee and an adulterant (either roasted maize flour or soybean flour) were prepared from each brand of ground roasted coffee with the proportions of roasted maize or soybean flours added into the coffee powders from 5 to 40 wt% with a step of 5% (together 8%). The obtained binary mixtures were thoroughly stirred and vortexed to ensure homogeneity. Proportions > 40% were not considered since the admixture of the adulterant above this percentage was sensory evident. For each brand of coffee, 3 replicates were performed. Accordingly, a total of 288 adulterated ground coffee samples were obtained (6 biological replicates \times 2 adulterants \times 3 technical replicates \times 8%).

2.2 FFSFS measurement

Front-face fluorescence spectra were acquired by an FS5 spectrofluorometer (Edinburgh, Livingston, Scotland,

Britain) with a 150 W xenon lamp source and an SC-10 front-face sample holder at room temperature (25 °C). The incidence angle of the excitation radiation was 30° which was fixed by the holder. The slit widths for excitation and emission were both 3 nm. Seventy milligrams of samples were mounted in the sample holder. Excitation and emission were scanned simultaneously with a constant wavelength interval ($\Delta\lambda$) between excitation wavelength (λ_{ex}) and emission wavelength (λ_{em}). Synchronous fluorescence spectra were collected in the range of λ_{ex} from 240 to 600 nm and $\Delta\lambda$ from 30 to 200 nm, and the steps for λ_{ex} and $\Delta\lambda$ were 1 and 10 nm, respectively. The wavelength scanning speed was 100 nm/s. The estimated time to obtain the total synchronous fluorescence spectra of a measurement was 1.5 min (the scanning time = 360 nm of λ_{ex} range / 100 nm/s of scanning speed \times 18 $\Delta\lambda$ = 65 s, and the switching time between every two $\Delta\lambda$ was 1–2 s). To minimize measurement error, the spectra were measured 3 times successively for each sample, and the average was pretreated by Savitzky–Golay smoothing through 7 points as an embedded default function in the FS5 spectrofluorometer software “Fluoracle” (Edinburgh, Livingston, Scotland, Britain). The smoothed spectral data were then auto-scaled 7 times, in order to give variables with zero means/unit a standard deviation.

2.3 Multivariate calibration and validation

Prior to statistical analysis, several commonly used spectral data pretreatments including peak or area normalization, standard normal variate (SNV), multiplicative scatter correction (MSC), first (1st) and second (2nd) derivative preprocesses were tested. Principal component analysis (PCA) and linear discriminant analysis (LDA) were executed by SPSS 19.0 (IBM, Armonk, NY, USA). PLSR was performed by Unscrambler X 10.4 (CAMO, Oslo, Norway).

Limited by the maximal variable number of SPSS 19.0, the variable dimensionality needs a preliminary reduction. In our previous work on utilizing synchronous fluorescence spectroscopy for geographical discrimination of red wines (Tan et al. 2016), we found that $\Delta\lambda$ with intervals of 30 nm can provide supplementary chemical information, while $\Delta\lambda$ with less intervals (10 or 20 nm) will contain redundant data and greater intervals (> 60 nm) may omit some useful information. Accordingly, to reduce variable number and retain important information, the spectral data at every three $\Delta\lambda$ in the range of 30–200 nm (together six selected $\Delta\lambda$: 30, 60, 90, 120, 150, and 180 nm) of the 288 adulterated samples and 18 pure ground coffee samples were imported into the software as the variables for PCA ($n=306$). The yielded principal components (PCs) were used as variables for LDA. PCA–LDA qualitative models were optimized and validated by both full (*leave-one-out*) and fivefold cross-validations. The sensitivity (true positive rate) and specificity (true

negative rate) for each adulterant were calculated. The sensitivity was measured as the fraction of one type of adulterated samples which had a positive test result (correctly identified as containing the actual adulterant), while the specificity was calculated as the fraction of the other samples which had a negative test result (correctly recognized as not containing the adulterant).

After qualitative discrimination, the PLSR prediction models for each adulterant were constructed individually with 18 unadulterated coffee samples, and 144 adulterated samples constituted the calibration set ($n=162$). The PLSR models were validated by both fivefold cross-validation and external validation. For fivefold cross-validation, all the samples were split into five segments of similar size. Then one selected segment was left out as an evaluation set, while the remaining four segments were utilized to generate classification rules. This process was repeated five times until each segment was left out once. The corresponding root mean square error of calibration (RMSEC), coefficient of determination for calibration (R^2_c), root mean square error of cross-validation (RMSECV) and coefficient of determination for cross-validation (R^2_{cv}) were determined. The optimal number of PLSR latent variables was revealed by plotting the RMSECV vs. the number of latent variables and determining the minimum for the plot. For external validation, every 5 of samples were injected into a test set ($n=32$), while the remaining samples composed a training set ($n=130$). The RMSEP and corresponding R^2_p were calculated. The REP was calculated as the percentage ratio of the RMSEP to the mean of the actual content values. Standard error of prediction (SEP), RPD, and range error ratio (RER) as the standard deviation ratio of the reference values and the range of reference values to RMSEP, respectively, were also determined. The LOD were calculated according to Allegrini and Olivieri (2014) and Márquez et al. (2019) at the 95% confidence level.

2.4 Simulated blind sample test

Finally, a simulated blind sample test was performed to assess the reliability of the built models. Ground coffee samples ($n=6$) were added with different proportions of roasted maize or soybean flour into a blank ground coffee sample. The spiking proportions included high (36% or 38%), medium (26%), and low levels (14%). The spiked samples were mixed homogeneously, scanned by FFSFS and predicted by the strategy of PCA–LDA coupled with PLSR, parallel to model calibrations. Three replicates were performed for each spiked sample. Relative error was calculated as the average percentage of the difference between the predicted and the actual values.

3 Results and discussion

3.1 FFSFS of ground roasted Arabica coffee

The FFSFS properties of all pure coffee and cereal flour samples were first investigated and compared. The FFSFS contour maps of the six ground roasted Arabica coffee samples exhibited high similarity (Fig. S1, Supplementary Material). Compared to green coffee beans, the fluorescence properties of ground roasted coffee presented dramatic modifications. The characteristic emissions from phenolic acids (typically caffeic acid), flavonoids (typically quercetin), and the lipid fraction (typically tocopherol) in green coffee beans, mainly in the range of $\lambda_{\text{ex}} = 250\text{--}500$ nm (Botelho et al. 2017; Robert et al. 2022), all nearly disappeared in the maps of ground roasted coffee. Instead, there was a strong and broad fluorescence emission at relatively larger λ_{ex} (500–600 nm). This wide-ranging band is likely the combination of multiple fluorescent species of similar structure and property. Considering the major components in roasted coffee, it is assumed to primarily belong to the fluorescent Maillard reaction products, i.e., melanoidins (Matiacevich et al. 2005). However, as the product composition of the Maillard reaction in roasted products is complicated and the chemical structures of most advanced glycosylation end products are still unknown (Matiacevich et al. 2005), the direct acknowledgement of this fluorescence band to specific fluorophores cannot be achieved.

In addition to this strong and broad emission at relatively larger λ_{ex} , some weak bands were found at relatively lower $\lambda_{\text{ex}} < 300$ nm. We have observed the front-face fluorescence emissions of caffeine and theobromine in dark chocolate in this area (Tan et al. 2019). Although the level of caffeine is only as low as approx. 1 mg/g in dark chocolate, its fluorescence is easy to recognize in the contour maps of dark chocolate, since the two methylxanthines are the dominant fluorophores in dark chocolate. On the contrary, though the caffeine content in coffee normally can reach to approximately 1.3% (Feldman et al. 1969), its fluorescence was far from that obvious as in dark chocolate. As the predominant fluorescent species in roasted coffee is the aforementioned Maillard reaction products, the fluorescence of caffeine is much weaker and seems very obscure at the magnitude of the fluorescence of Maillard reaction products.

To confirm the attribute of fluorescence emission in the range of $\lambda_{\text{ex}} < 300$ nm, a typical ground roasted coffee sample was spiked with 2%, 5% and 10% caffeine (Fig. 1a–d). The contour map of pure solid caffeine is also shown in Fig. 1e for comparison. Along with the increase of the spiked concentration of caffeine from 2 to 10%, the fluorescence emission $< \lambda_{\text{ex}} = 300$ nm gradually became stronger and clearer, suggesting that the emission did come from

caffeine (Fig. 1). However, the emission of pure caffeine with $\lambda_{\text{ex}} = 320\text{--}380$ nm (Fig. 1e) never appeared in the maps of the spiked samples (Fig. 1a–d). This concentration-dependent fluorescence behavior agrees well with the so-called aggregation-induced emission (AIE), which is described to be an unusual ratio of photophysical phenomenon and solution state. Or the fluorescent emission is induced by aggregate formation, either in solution or solid state (Luo et al. 2001). Accordingly, the emissions of caffeine at $\lambda_{\text{ex}} = 320\text{--}380$ nm only occurred when it was in pure solid or highly aggregated state (a concentration of 10% is insufficient). Actually, a similar phenomenon was also observed by us (Tan et al. 2019). The solid caffeine emissions at $\lambda_{\text{ex}} = 320\text{--}380$ nm could not be found in the spectra of dark chocolates (where caffeine content is $< 0.2\%$) (Tan et al. 2019). Even at 10%, aggregated caffeine could still not yield at $\lambda_{\text{ex}} = 320\text{--}380$ nm, not to mention the caffeine levels in coffee and chocolate which are far $< 10\%$. The precise mechanism and condition of the AIE of caffeine is currently under our investigation.

3.2 FFSFS of roasted maize and soybean flours

Figure 2 shows the contour maps of soybean and maize flours before and after roasting. The FFSFS emissions for fresh unroasted soybean and maize flours have been well documented (Karoui et al. 2006; Zeković et al. 2012; Xue et al. 2021). They can roughly be divided into 3 regions (Figs. 2a and 2b). The first band ($\lambda_{\text{ex}} = 250\text{--}300$ nm) is of strongest fluorescence intensity, contributed largely by tryptophan. The second band ($\lambda_{\text{ex}} = 300\text{--}400$ nm) is primarily due to the emissions of other phenolic acids such as chlorogenic acid. The third band was only found in soybean flour at $\lambda_{\text{ex}} = 400\text{--}500$ nm and mainly belongs to soy isoflavones. After roasting, these 3 emission regions all disappeared and were replaced by a new broad region at $\lambda_{\text{ex}} = 450\text{--}600$ nm. Similar to roasted coffee, this region is supposed to be ascribed to fluorescent Maillard reaction products.

Although no standard melanoidin is available for spiking experiments which could verify our assumption like for caffeine, an experiment was designed to support the hypothesis from another angle. Tanaka et al. (2008) found that the Maillard reaction is faster when the water activity (A_w) is between 0.4 and 0.7, while higher or lower A_w will reduce the rate of the Maillard reaction. Accordingly, before roasting, the soybean flour was thoroughly dried in an oven at 105 °C until a constant weight to reduce A_w and decelerate the Maillard reaction. The Fig. 2c, e show the comparison of the contour maps of the roasted soybean flours with and without pre-drying process. The fluorescence intensity of the soybean flour, which was roasted after drying, was significantly lower than that of the undried one, while its general emission band shape kept unaltered. Replacing soybean flour

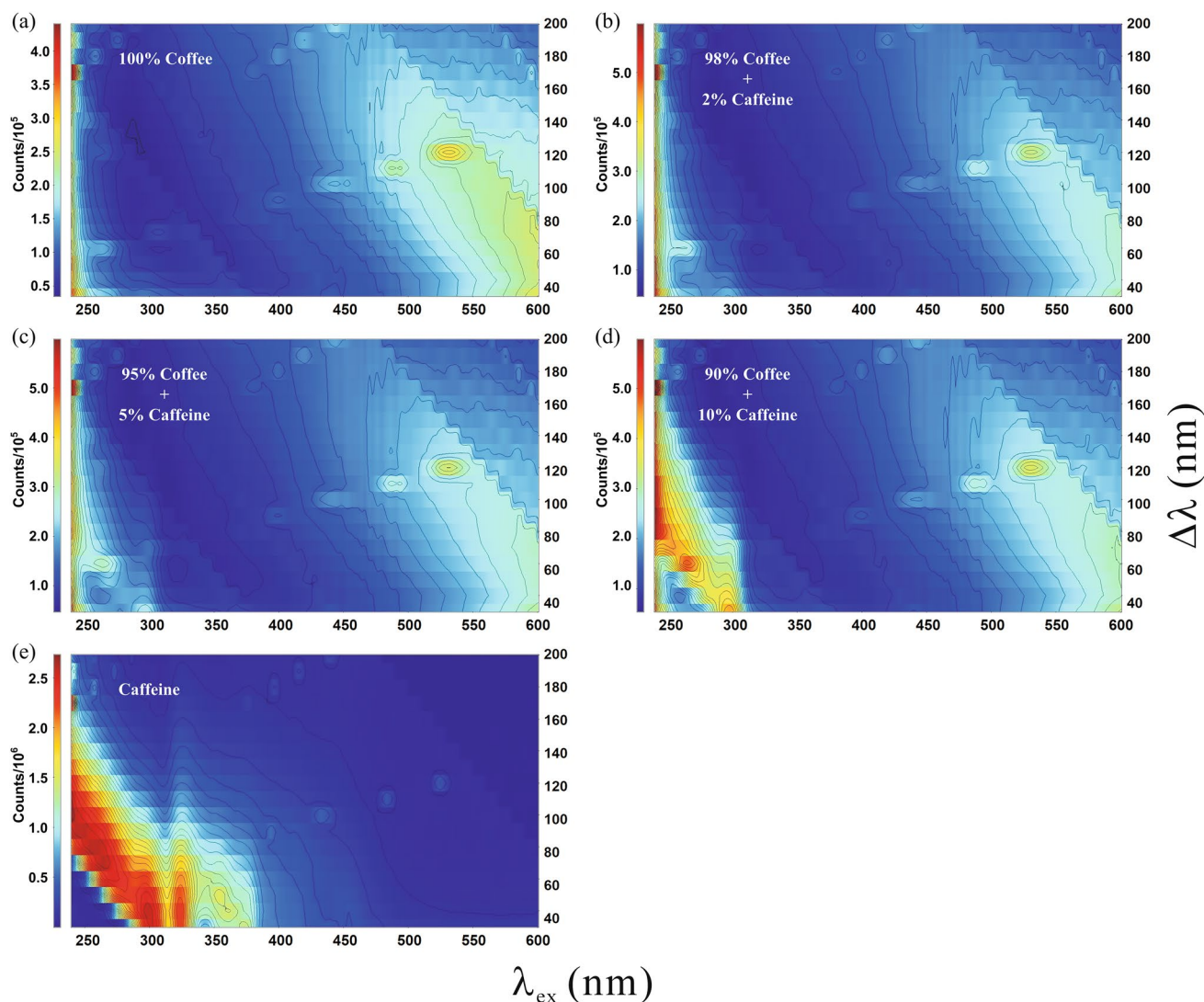


Fig. 1 Contour maps for the total front-face synchronous fluorescence spectra of **a** a typical ground roasted Arabica coffee sample, the coffee sample **a** spiked with different proportions of solid caffeine:

b 2% caffeine+98% coffee; **c** 5% caffeine+95% coffee; **d** 10% caffeine+90% coffee, and **e** pure solid caffeine

by maize flour lead to a similar phenomenon. Thus, this supports to some extent our assumption that the broad emission band derives from the Maillard products. However, it should be noted that owing to the light color of this roasted but pre-dried soybean flour, it was not suitable for adulteration. Consequently, roasting without pre-drying was adopted for the study of adulteration detection.

At first glance, the contour maps of roasted coffee (Fig. 1a), roasted soybean (Fig. 2c) and maize (Fig. 2d) flours seem rather analogous. However, their band center positions and intensities differ from each other. As aforementioned, roasted Arabica coffees presented maximal emission around $\lambda_{\text{ex}} = 600$ nm and $\Delta\lambda = 40\text{--}80$ nm. Compared to roasted coffee, the spectra of roasted cereal flours showed hypsochromic shifts. For roasted maize flour, the maximal emission

centered at $\lambda_{\text{ex}} = 500\text{--}550$ nm and $\Delta\lambda = 100\text{--}140$ nm, while roasted soybean flour emitted rather strong fluorescence at $\lambda_{\text{ex}} = 550\text{--}600$ nm and $\Delta\lambda = 60\text{--}100$ nm. Besides, the band of roasted soybean flour was significantly stronger than that of maize flour. The band shape of roasted coffee had a high resemblance to the one of roasted soybean flour. However, it was much weaker than the soybean flour band, similar to the maize flour band. The slightly different locations of emission bands of the three kinds of roasted samples are probably due to their dissimilar profiles of the Maillard reaction precursors, i.e., carbohydrates and proteins. The much higher fluorescent intensity of roasted soybean flour may stem from its extremely high contents of protein, which was also the reason why the roasting temperature for soybean flour was lower than in maize flour. These differences are directly

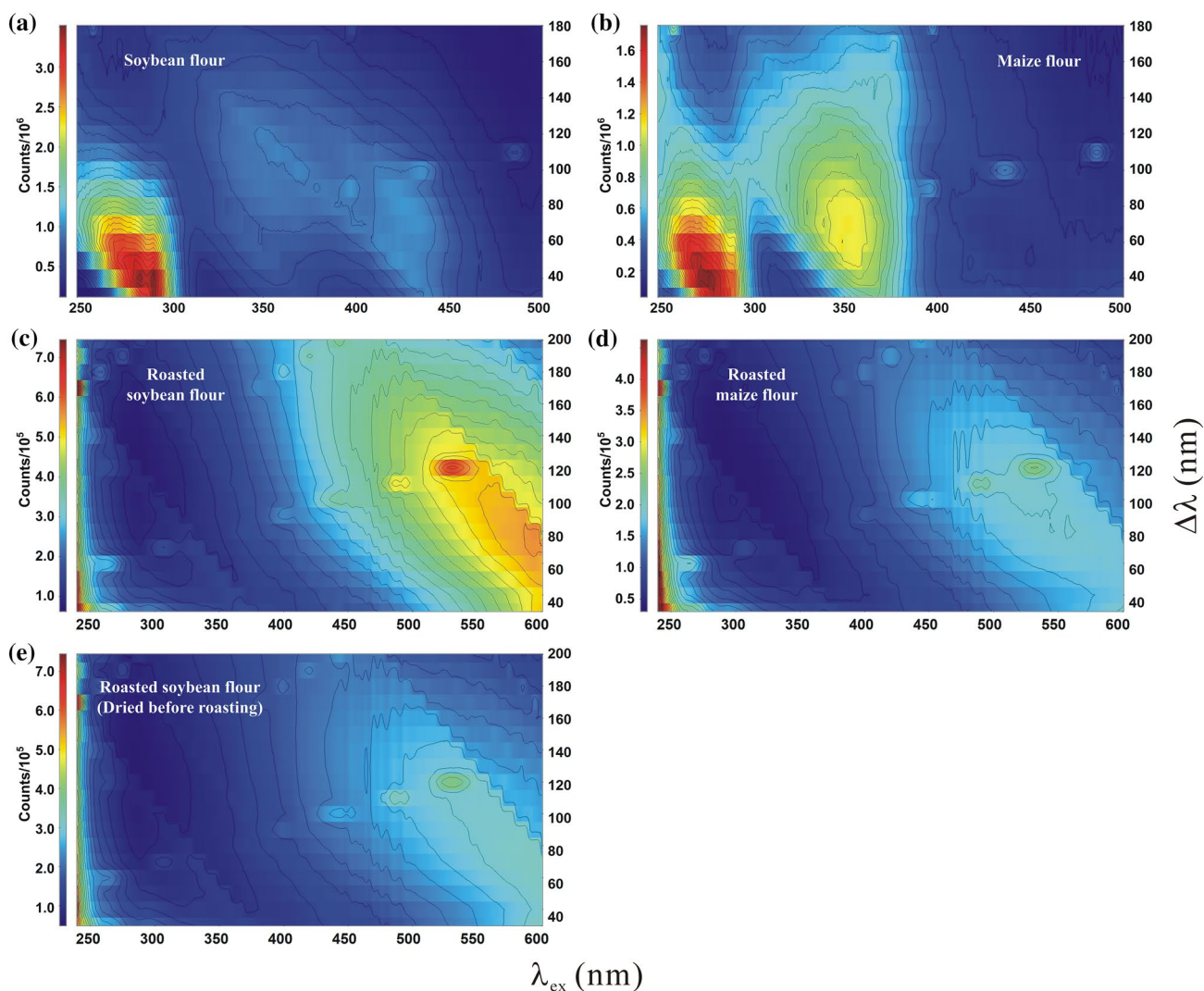


Fig. 2 Contour maps for the total front-face synchronous fluorescence spectra of **a** unroasted soybean flour, **b** unroasted maize flour, **c** roasted soybean flour, **d** roasted maize flour and **e** roasted soybean flour which was dried in an oven at 105 °C until a constant weight prior to roasting

reflected in the fluorescence behaviors in FFSFS. Hence, owing to the unique characteristics belonging to different botanical origins, each contour map presents a distinctive fluorescence “fingerprint”, which can be utilized for analysis purposes. Although such “fingerprints” of roasted coffee and cereal flours are hardly distinguishable by the naked eye, the tiny difference between them can be enlarged by data pretreatment and multivariate statistical analysis.

3.3 FFSFS of adulterated coffee

The contour plots of a typical ground roasted coffee adulterated with different proportions of roasted soybean flour are shown in Fig. 3. As expected, the emission bands of the binary blends displayed regular changes as the proportion of roasted soybean flour increased. The band did not alter

its shape, but its intensity gradually strengthened, especially when the content of soybean flour reached 15%. One should consider that the fluorescence intensity of roasted soybean flour is higher than that of roasted ground coffee.

As shown in Fig. S2 (Supplementary Material), roasted maize flour as the adulterant is different. As the fluorescence intensity of roasted maize flour was comparable to that of ground roasted coffee, the intensity of their mixtures did not change significantly. Yet with the increase of roasted maize flour proportion, the emission bands of the binary mixtures showed a gradual blue shift, though only to a slight extent. In general, as the adulteration proceeded, the contour map of the mixture gradually resembled the pattern of the adulterant, and the specific tendency was dependent on the certain adulterant. These results provide the basis for the

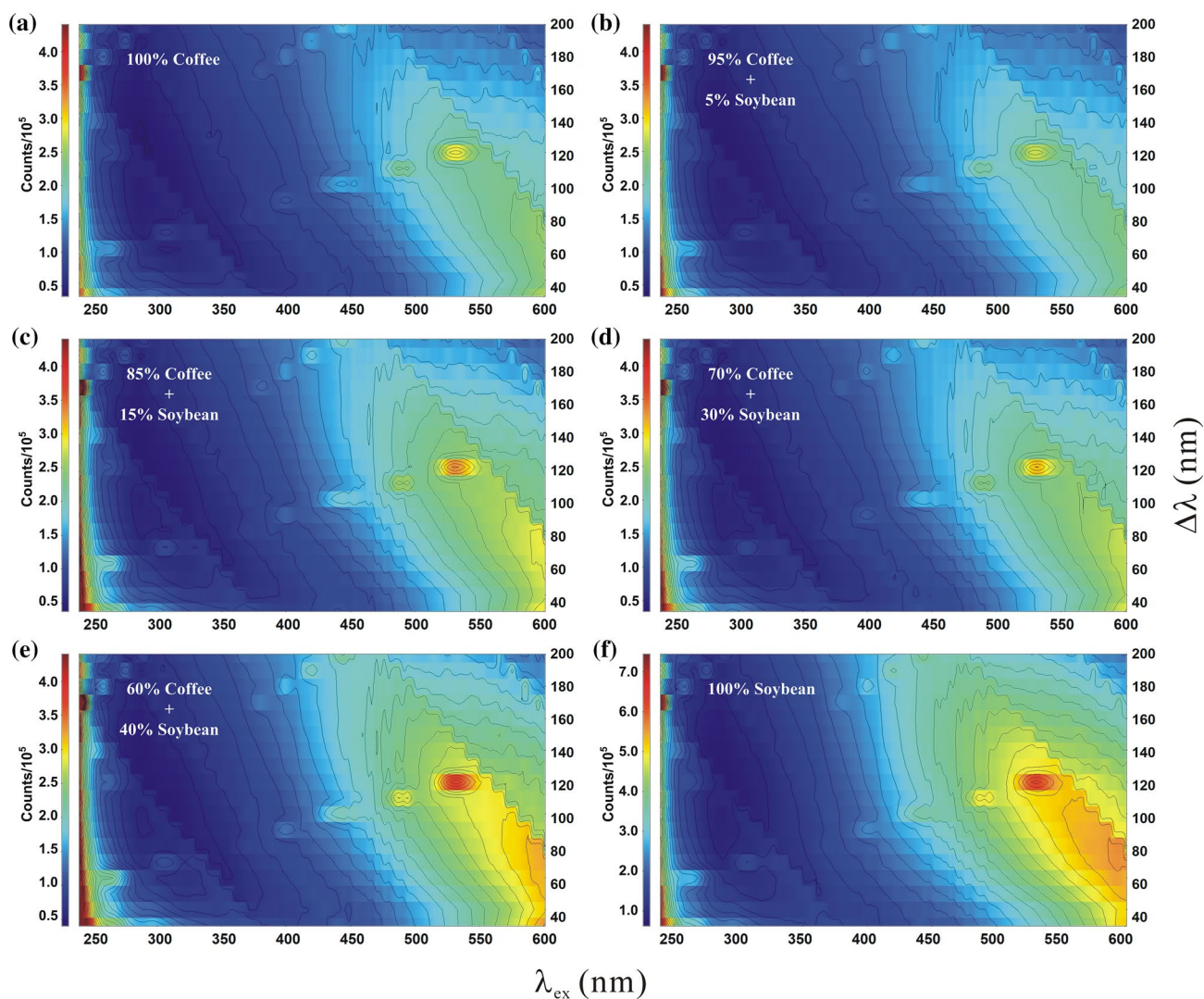


Fig. 3 Contour maps for the total front-face synchronous fluorescence spectra ($\lambda_{\text{ex}}=240\text{--}600$ nm and $\Delta\lambda=30\text{--}200$ nm) of **a** a typical ground roasted Arabica coffee sample, the coffee sample **a** adulter-

ated with different proportions **b** 5%; **c** 15%; **d** 30%; **e**, 40% of roasted soybean flour, and **f** the adulterant roasted soybean flour

qualitative and quantitative detection of two adulterants in ground roasted coffee.

3.4 PCA-LDA discrimination

Prior to statistical analysis, synchronous fluorescence spectra were pretreated by SNV to eliminate the influence of moisture to a certain degree. In this study, it was superior to other data pre-treatments including normalization, MSC, 1st and 2nd derivatives. Then, first PCA was performed to reduce variable dimensionality and for preliminary discrimination. As each sample's total synchronous fluorescence data was in form of a 3D matrix ($x: \lambda_{\text{ex}}$; $y: \Delta\lambda$; z : intensity), it was run at λ_{ex} from 240 to 600 nm, step = 1 nm; $\Delta\lambda = 30, 60, 90, 120, 150, \text{ and } 180$ nm; intensity at each pair of λ_{ex} and $\Delta\lambda$

for each sample, along with sequentially increasing $\Delta\lambda$ and concatenated for a vector data type suitable for PCA ($x: \lambda_{\text{ex}}$ at successive $\Delta\lambda$; y : intensity). Accordingly, the first 361 variables for each sample were the intensities λ_{ex} from 240 to 600 nm and $\Delta\lambda = 30$ nm; the following second 361 variables were at λ_{ex} from 240 to 600 nm and $\Delta\lambda = 60$ nm; etc. until the last 361 variables were λ_{ex} from 240 to 600 nm and $\Delta\lambda = 180$ nm. Eventually, 2166 variables ($361 \times 6 \Delta\lambda$) were yielded for each sample. All samples' unfolded data were imported into the SPSS software for the following PCA. The obtained PC scores were plotted as 2D PCA score plots (Fig. S3a, Supplementary Material). PC1 and PC2 accounted for 64.7% and 20.0% of total variance, respectively (together more than 80% of cumulative variance). The PCA could not clearly distinguish between the unadulterated and the two

adulterated coffees. To disclose underlying variables, PC loadings were refolded into 3D matrices ($x: \lambda_{ex}$; $y: \Delta\lambda$; z : loading). The first 2 PC loadings were calculated to create a contour map for variable selection (Figs. S3c and S3d, Supplementary Material). The loading plot of PC1 was largely overlapping with the emission of fluorescent Maillard reaction products, while the PC2 loadings corresponded to caffeine at $\lambda_{ex} = 240\text{--}300$ nm. The two loading plots together covered almost the full range of λ_{ex} and $\Delta\lambda$, indicating that the total synchronous fluorescence data are suitable for discrimination. At that point, the first two PCs were selected as the variables for LDA and the unfolded total synchronous fluorescence data ($x: \lambda_{ex}$ at different $\Delta\lambda$; y : intensity) were employed in PLSR.

After dimensionality reduction, LDA was executed according to 3 categories:

1. unadulterated ground roasted coffee,
2. ground roasted coffee adulterated with roasted maize flour,
3. ground roasted coffee adulterated with roasted soybean flour.

Compared to the strong overlap in the PCA score plot, the supervised recognition method LDA showed an improved separation (Fig. S3b, Supplementary Material). Although the separation of the 3 categories was still not complete, most of them could be distinguished from each other. Considering that the LDA classification was based on the yielded PCs, the first 2 that account for 64.7% and 20.0% of total variance were related to fluorescent Maillard reaction products and caffeine, respectively. Though they are highly analogous and hard to differentiate, a slight discrepancy among them

may be the composition of fluorescent Maillard reaction products and caffeine. The validation of LDA gave suitable discrimination results. The cross-validated sensitivity (true positive rate) and specificity (true negative rate) of roasted maize and soybean flours were at least 88.9% (Table S1, Supplementary Material).

3.5 PLSR prediction

After roasting, the color and appearance of soybean and maize flours were extremely close to those of ground roasted coffee. For consumers, the discrepancy between adulterated and non-adulterated coffee is difficult to discern by naked eye and taste, as long as the proportion of roasted maize or soybean flour in binary blends does not exceed 40%. After the qualitative identification of an adulterant, the proportion was predicted by PLSR (Fig. 4), using the calibration model for each adulterant separately. The resulting calibration and validation characteristics are listed in Table 1. For calibration, fivefold cross-validation and external validation, the R^2 values were in the range of 0.90–0.96 and the RMSE were at most 3.9%. The REP were 20.1% and 17.3% and the corresponding RPD were 3.5 and 3.9 for roasted maize and soybean flour, respectively. Although the RPD values did not reach 5.0, the values > 3.1 were sufficient to demonstrate the feasibility of the model when used for screening purpose.

The LOD for roasted maize and soybean flours was 10%, respectively. On the global market, the common ratios of coffee adulteration by roasted cereal flours are unknown. The adulteration ratios in the literature range between 2 and 50% for roasted soybean and maize flours in coffee (Arrieta et al. 2019; Cai et al. 2016; Daniel et al. 2018). One study

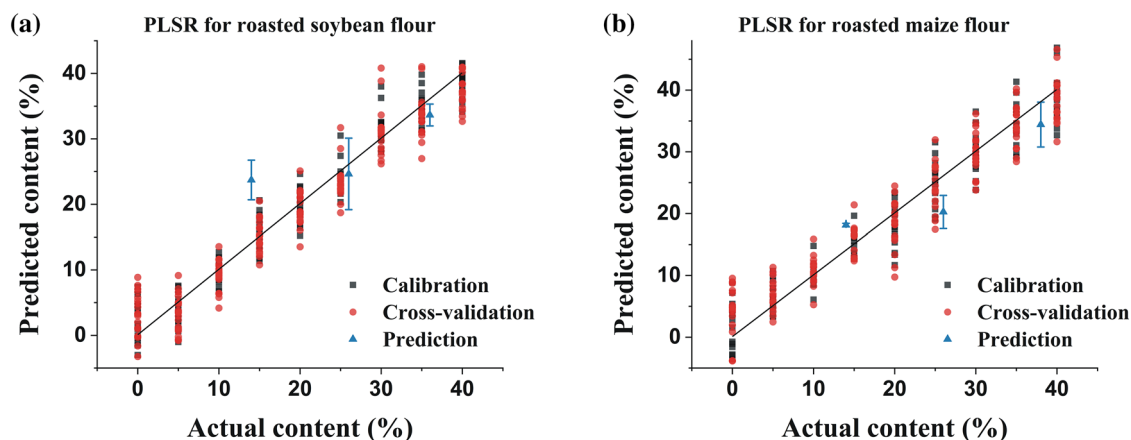


Fig. 4 PLSR predicted vs. actual content of roasted soybean and maize flours adulterants in ground roasted Arabica coffee based on unfolded total front-face synchronous fluorescence spectra under opti-

mal conditions as shown in Table 1. Blue triangles with error bars (mean \pm s; $n=3$) represent simulated blind samples in Table 2

Table 1 PLSR statistics for the determination of the adulterated roasted maize and soybean flours in ground roasted Arabica coffee using total unfolded front-face synchronous fluorescence spectra ($\lambda_{ex} = 240\text{--}600\text{ nm}$; $\Delta\lambda = 30\text{--}200\text{ nm}$)

Parameter	Maize flour	Soybean flour
No. of LV ^a	7	7
R^2_c ^b	0.948	0.952
RMSEC (%) ^c	3.2	3.1
R^2_{cv} ^d	0.945	0.950
RMSECV (%) ^e	3.3	3.2
R^2_p ^f	0.904	0.933
RMSEP (%) ^g	3.9	3.2
REP (%) ^h	20.1	17.3
Prediction bias (%)	0	0
SEP (%) ⁱ	3.6	3.1
RPD ^j	3.5	3.9
RER ^k	8.9	10
LOD (%) ^l	10.0	10.0

^aNo. of LV, number of latent variables
^b R^2_c , determination coefficient of calibration
^cRMSEC, root mean square error of calibration
^d R^2_{cv} , determination coefficient of five-fold cross-validation
^eRMSECV, root mean square error of five-fold cross-validation
^f R^2_p , determination coefficient of prediction
^gRMSEP, root mean square error of prediction
^hREP (%), relative error of prediction
ⁱSEP, standard error of prediction
^jRPD, ratio of the SD of reference values to RMSEP
^kRER, ratio of reference amplitude to RMSEP
^lLOD, limit of detection

that used an ultra-performance liquid chromatography-high resolution mass spectrometry reported a LOD of 5% for soybean flour (Cai et al. 2016). And while the LOD in this study was slightly higher, the method was faster and simpler, and more importantly, non-destructive and cost-effective. Therefore, it may be particularly suitable for preliminary

screening of roasted coffee adulteration with large amounts of roasted cereal flours.

3.6 Simulated blind sample test

To further validate the applicability of the proposed method, simulated blind sample tests were executed. Several unknown ground roasted coffee samples spiked with roasted maize or soybean flour were analyzed by the optimized prediction model. Both Table 2 and Fig. 4 show the results of PLSR prediction and the comparison with the actual values. The models yielded suitable results, with the majority of the calculated relative errors ranging between -30 and $+30\%$, except for one coffee sample containing 14% roasted soybean flour showing a large error of 69%. In the triplicate measurements of this sample, the coefficient of variation was not significantly higher than in other samples (12.7%), indicating that those 69% did not stem from an accidental error. The large error may be due to the systematic error towards relatively low adulteration proportions. In fact, when the adulteration proportions were adjacent to the method LOD (14%), the relative errors increased, i.e., the models would give over-estimated prediction values. For the coffee sample containing 14% roasted maize flour, the relative error was 29%. While the adulteration proportions were much higher than LOD ($> 20\%$), the relative errors decreased to negative levels that were acceptable (-22 to -5%). This result shows a limited applicability of the method for adulterated coffee samples with relatively low adulteration proportions.

The results of the model construction and simulated blind sample tests demonstrate that the proposed method is suitable for a real application as rapid adulteration screening of ground roasted coffee with roasted maize and soybean flours. However, the number of original products used in this study for the construction of sample sets was insufficient. Consequently, more representative samples from different geographical origins, cultivars, and harvest years should be collected and calibrated to construct a more robust and reliable model for real application. Unfortunately, owing to

Table 2 Results for the analysis of 6 simulated blind samples (mean \pm s; n = 3)

Sample	Actual value (%)		Predicted value (%)		Relative error (%)
	Maize flour	Soybean flour	Maize flour	Soybean flour	
1	14.0	0	18.1 \pm 0.3	–	29
2	26.0	0	20.2 \pm 2.6	–	–22
3	38.0	0	34.4 \pm 3.6	–	–9
4	0	14.0	–	23.7 \pm 3.0	69
5	0	26.0	–	24.6 \pm 5.4	–5
6	0	36.0	–	33.7 \pm 1.6	–7

Relative error was calculated as the average percentage of the difference between the predicted and the actual values

the COVID-19 pandemic, the commercial availability of original items is largely restricted and the above improvements can only be made in future works.

4 Conclusion

This study shows a fast and non-invasive detection of roasted maize and soybean flours in ground roasted Arabica coffee by the combined use of FFSFS and multivariate statistical analysis. The fluorescence properties of roasted coffee changed significantly compared to the ones of green coffee beans. The dominant fluorophores in roasted coffee are assumed to be fluorescent Maillard reaction products, followed by caffeine. The FFSFS of the cereal flours also changed considerably after roasting. However, they were different from the FFSFS of roasted coffee. PCA-LDA and PLSR were suitable for qualification and quantification of the two adulterants. Our results demonstrate that FFSFS has the potential to detect > 10% roasted maize and soybean flours in ground roasted coffee for a rapid adulteration control. This capability may originate from the differences in the profiles of carbohydrate, protein, and caffeine between coffee and cereal flours before roasting, and hence the composition of fluorescent Maillard reaction products and caffeine after roasting. The benefits of this method are convenience, rapidity and non-destructive detection. However, owing to the high similarity in FFSFS of ground roasted coffee and roasted maize and soybean flours, this proposed method is not capable to determine an adulteration < 10%. Besides, because different coffee roasting conditions will affect the amount of fluorescent Maillard products, the applicability of the proposed method is limited to the analysis of coffees containing adulterants with the same roasting degree, e.g., medium roasted coffee adulterated with roasted cereal flours to an analogous color. Nevertheless, it introduces a new tool to understand the food deteriorative reactions after heating treatment.

Supplementary Information The online version contains supplementary material available at <https://doi.org/10.1007/s00003-022-01396-8>.

Author contributions JYX: methodology, investigation, software, visualization, writing—original draft. JT: conceptualization, methodology, visualization, writing—review and editing.

Funding This research did not receive any specific grant from funding agencies in the public, commercial, or not-for-profit sectors.

Declarations

Conflict of interest The author declares that they have no conflict of interest.

References

- Allegrini F, Olivieri AC (2014) IUPAC-consistent approach to the limit of detection in partial least-squares calibration. *Anal Chem* 86:7858–7866
- Arrieta AA, Arrieta PL, Mendoza JM (2019) Analysis of coffee adulterated with roasted corn and roasted soybean using voltammetric electronic tongue. *Acta Sci Pol Technol Aliment* 18(1):35–41
- Bilge G (2020) Investigating the effects of geographical origin, roasting degree, particle size and brewing method on the physicochemical and spectral properties of Arabica coffee by PCA analysis. *J Food Sci Technol* 57:3345–3354
- Botelho BG, Oliveira LS, Franca AS (2017) Fluorescence spectroscopy as tool for the geographical discrimination of coffees produced in different regions of Minas Gerais State in Brazil. *Food Control* 77:25–31
- Cai T, Ting H, Jin-lan Z (2016) Novel identification strategy for ground coffee adulteration based on UPLC–HRMS oligosaccharide profiling. *Food Chem* 190:1046–1049
- Callao MP, Ruisánchez I (2018) An overview of multivariate qualitative methods for food fraud detection. *Food Control* 86:283–293
- Chakravartula SSN, Moscetti R, Bedini G, Nardella M, Massantini R (2022) Use of convolutional neural network (CNN) combined with FT-NIR spectroscopy to predict food adulteration: a case study on coffee. *Food Control* 135:108816. <https://doi.org/10.1016/j.foodcont.2022.108816>
- Danezis GP, Tsagkaris AS, Brusica V, Georgiou CA (2016a) Food authentication: state of the art and prospects. *Curr Opin Food Sci* 10:22–31
- Danezis GP, Tsagkaris AS, Camin F, Brusica V, Georgiou CA (2016b) Food authentication: techniques, trends & emerging approaches. *TrAC Trends Anal Chem* 85:123–132
- Daniel D, Lopes FS, dos Santos VB, do Lago CL (2018) Detection of coffee adulteration with soybean and corn by capillary electrophoresis-tandem mass spectrometry. *Food Chem* 243:305–310
- Domingues DS, Pauli ED, de Abreu JE, Massura FW, Cristiano V, Santos MJ, Nixdorf SL (2014) Detection of roasted and ground coffee adulteration by HPLC and by amperometric and by post-column derivatization UV-Vis detection. *Food Chem* 146:353–362
- Ebrahimi-Najafabadi H, Leardi R, Oliveri P, Casolino MC, Jalali-Heravi M, Lanteri S (2012) Detection of addition of barley to coffee using near infrared spectroscopy and chemometric techniques. *Talanta* 99:175–179
- Feldman RS, Ryder WS, Kung JT (1969) Importance of nonvolatile compounds to the flavor of coffee. *J Agric Food Chem* 17(4):733–739
- Garrett R, Vaz BG, Hovell AM, Eberlin MN, Rezende CM (2012) Arabica and Robusta coffees: identification of major polar compounds and quantification of blends by direct-infusion electrospray ionization-mass spectrometry. *J Agric Food Chem* 60(17):4253–4258
- Karoui R, Blecker C (2011) Fluorescence spectroscopy measurement for quality assessment of food systems—a review. *Food Bioproc Technol* 4(3):364–386
- Karoui R, Cartaud G, Dufour E (2006) Front-face fluorescence spectroscopy as a rapid and nondestructive tool for differentiating various cereal products: a preliminary investigation. *J Agric Food Chem* 54(6):2027–2034
- Luo J, Xie Z, Lam JWY, Cheng L, Chen H, Qiu C, Kwok HS, Zhan X, Liu Y, Zhu D, Tang BZ (2001) Aggregation-induced emission of 1-methyl-1,2,3,4,5-pentaphenylsilole. *Chem Commun* 18:1740–1741
- Márquez C, Ruisánchez I, Callao MP (2019) Qualitative and quantitative multivariate strategies for determining paprika adulteration with Sudan I and II dyes. *Microchem J* 145:686–692

- Matiacevich SB, Santagapita PR, Buera MP (2005) Fluorescence from the Maillard reaction and its potential applications in food science. *Crit Rev Food Sci Nutr* 45:483–495
- Reis N, Franca AS, Oliveira LS (2013a) Discrimination between roasted coffee, roasted corn and coffee husks by Diffuse Reflectance Infrared Fourier Transform Spectroscopy. *LWT - Food Sci Technol* 50(2):715–722
- Reis N, Franca AS, Oliveira LS (2013b) Performance of diffuse reflectance infrared Fourier transform spectroscopy and chemometrics for detection of multiple adulterants in roasted and ground coffee. *LWT Food Sci Technol* 53:395–401
- Reis N, Botelho BG, Franca AS, Oliveira LS (2017) Simultaneous detection of multiple adulterants in ground roasted coffee by ATR-FTIR spectroscopy and data fusion. *Food Anal Methods* 10:2700–2709
- Robert JV, de Gois JS, Rocha RB, Luna AS (2022) Direct solid sample analysis using synchronous fluorescence spectroscopy coupled with chemometric tools for the geographical discrimination of coffee samples. *Food Chem* 371:131063. <https://doi.org/10.1016/j.foodchem.2021.131063>
- Tan J, Li R, Jiang ZT, Zhang Y, Hou YM, Wang YR, Wu X, Gong L (2016) Geographical classification of Chinese Cabernet Sauvignon wines by data fusion of UV–visible and synchronous fluorescence spectroscopies: the combined use of multiple wavelength differences. *Aust J Grape Wine R* 22:358–365
- Tan J, Li R, Jiang ZT, Tang SH, Wang Y (2019) Rapid and non-destructive prediction of methylxanthine and cocoa solid contents in dark chocolate by synchronous front-face fluorescence spectroscopy and PLSR. *J Food Compos Anal* 77:20–27
- Tanaka M, Chiba N, Ishizaki S, Takai R, Taguchi T (2008) Influence of water activity and Maillard reaction on the polymerization of myosin heavy chain in freeze-dried squid meat. *Fish Sci* 60(5):607–611
- Toci AT, Farah A, Pezza HR, Pezza L (2016) Coffee adulteration: more than two decades of research. *Crit Rev Anal Chem* 46(2):83–92
- Wang X, Lim LT, Fu Y (2020) Review of analytical methods to detect adulteration in coffee. *J AOAC Int* 103(2):295–305
- Xue SS, Tan J, Xie JY, Li MF (2021) Rapid, simultaneous and non-destructive determination of maize flour and soybean flour adulterated in quinoa flour by front-face synchronous fluorescence spectroscopy. *Food Control* 130:108329. <https://doi.org/10.1016/j.foodcont.2021.108329>
- Yisak H, Redi-Abshiro M, Chandravanshi BS (2018) New fluorescence spectroscopic method for the simultaneous determination of alkaloids in aqueous extract of green coffee beans. *Chem Cent J* 12(1):59. <https://doi.org/10.1186/s13065-018-0431-4>
- Zeković I, Lenhardt L, Dramićanin T, Dramićanin MD (2012) Classification of intact cereal flours by front-face synchronous fluorescence spectroscopy. *Food Anal Methods* 5(5):1205–1213

Publisher's Note Springer Nature remains neutral with regard to jurisdictional claims in published maps and institutional affiliations.

Springer Nature or its licensor holds exclusive rights to this article under a publishing agreement with the author(s) or other rightsholder(s); author self-archiving of the accepted manuscript version of this article is solely governed by the terms of such publishing agreement and applicable law.